

Experimental Study on Seismic Performance of Equipment with Vibration Isolation Devices

Fan-Ru Lin, Jenn-Shin Hwang, Min-Fu Chen, Shiang-Jung Wang

NCREC (National Center for Research on Earthquake Engineering), Taiwan

Jenn-Shin Hwang, Jing-Wen Jeng

NTUST (National Taiwan University of Science and Technology), Taiwan



SUMMARY:

The earthquake resistant capacity of vibration-isolated equipment with spring isolators is seldom considered in practice. The purpose of this research is to study the seismic behavior of the spring isolators used for vibration isolation of a power generator. Both cyclic loading tests and shaking table tests were conducted to study the elastic and inelastic behavior of spring isolators. Testing results were preliminarily analyzed to investigate the damage mechanism and dynamic characteristics of the spring isolators. The appropriateness of the dynamic amplification factor specified in design codes for spring isolated equipment was discussed as well.

Keywords: spring isolators, shaking table test, cyclic loading test

1. INTRODUCTION

It is recognized that, to maintain functionality of an important building after an earthquake, both structural components and critical Mechanical/Electrical systems (M/E systems) should all perform well during the quake. However, several damaged cases during Chi-Chi and Hwa-Lien earthquakes of Taiwan have showed that spring isolated equipment, such as cooling towers, generators, and pumps, may be vulnerable earthquake loading (Fig. 1.1). In Taiwan, spring isolators are generally designed according to the weight and operating frequency of equipment, and the earthquake resistant capacity of vibration isolated equipment is however seldom considered in practice.



Figure 1.1. Leakage damage of a spring isolated cooling tower at the roof level after Hwa-Lien earthquake

According to field investigation results, open springs, housed springs and restrained springs were frequently used for mechanical equipment of M/E systems in hospitals and school buildings (Fig. 1.2). Recognizing the significance of the spring isolators in affecting the earthquake resistant capacity of critical M/E systems, a series of experimental studies were conducted by NCREC to investigate the seismic behavior of the commonly used spring isolators Taiwan. As shown in Fig. 1.3, seismic behavior of housed spring and restrained spring were previously studied (Hwang 2009). In order to simulate the practical dimensions of real equipment, the test bed sitting on spring isolators was

designed to deduce a width-to-height ratio of 30 for the vibration isolation systems. According to the test results, significant uplift response of the specimen with housed springs was observed. Thus, only restrained springs were suggested for practical applications in the earthquake prone area such as Taiwan. This study is then focused only at the seismic behaviour of the restrained springs. Meanwhile, considering the importance of emergency power supply after a major earthquake, an emergency generator was selected as the test specimen to observe realistic seismic responses of spring isolated equipment.



Figure 1.2. Commonly used spring isolator types in Taiwan

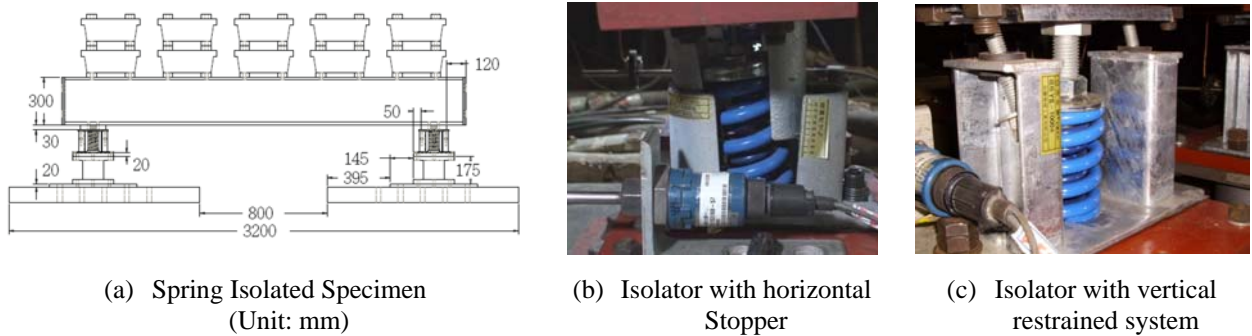


Figure 1.3. Test results of housed spring and restrained spring in previous study (Jenn-Shin Hwang 2009)

2. SEISMIC ISSUES IN TBC AND ASCE APPLICATIONS

In Taiwan Building Code (TBC, Ministry of the Interior 2011), the horizontal seismic design force F_{ph} of a vibration isolated generator is determined in accordance with Eq. (2.1):

$$F_{ph} = 0.4S_{DS}I_p \frac{a_p}{R_{pa}} \cdot (1 + 2h_x / h_n)W_p \quad (2.1)$$

where S_{DS} is the design spectral acceleration at short periods; I_p is the component importance factor for equipment or components; a_p is component amplification factor; R_{pa} is allowable component response reduction coefficient; h_x is the relative height to the ground of the story to which the equipment is located; h_n is the height of the building. From Eq. (2.1), it is obvious that the equation is similar to that given by ASCE 7-10 (ASCE 2010). One of the differences is the allowable component response reduction coefficient R_{pa} shown in Table 2.1. The other differences include: (1) in TBC, the vertical seismic force F_{pv} is defined by $1/2F_{ph}$ for general sites and $2/3F_{ph}$ for near-fault regions while F_{pv} is defined by $0.2S_{DS}W_p$ in ASCE 7-10. In this study, $0.2S_{DS}W_p$ was adopted as the vertical seismic design force; (2) Regarding the installation requirements for spring isolated components, SCE 7-10 suggests that isolated components should have horizontal restraints such as a bumper or snubber. To limit the

impact load, the gap between the support frame and restraint should not be greater than 6 mm; otherwise the horizontal seismic design force should be taken as $2F_{ph}$.

Table 2.1. Coefficients for vibration isolated generators.

System	Component	a_p		R_{pa} (R_p in ASCE 7-10)	
		TBC	ASCE 7-10	TBC	ASCE 7-10
Emergency Power Supply	Generators	1.0	1.0	2.0	2.5
Spring Isolated Generators		2.5	2.5	2.0	2.0

In the shaking table tests, tri-axial artificial input ground motions compatible with the RRS (Required Response Spectra) of AC-156 (ICC-ES, 2007) and TBC were used. The required horizontal and vertical spectral accelerations S_{ah} and S_{av} are given by Eq. (2.2):

$$\begin{aligned}
 S_{ah} &= 0.4S_{DS}a_p(1 + 2h_x/h_n) \\
 S_{av} &= 0.4 \cdot \left(\frac{2}{3}S_{DS}\right)a_p \quad \text{unit : } g
 \end{aligned} \tag{2.2}$$

Considering the code specifications in Taiwan, S_{DS} of the input motions was selected to be 0.8, and the equipment was assumed to be located at the basement or at roof level. For the case at roof level, ZPA (i.e. Zero Period Acceleration) of input motions in the horizontal and vertical directions were respectively equal to 0.96g and 0.21g according to AC-156 and TBC.

3. TEST PROGRAM

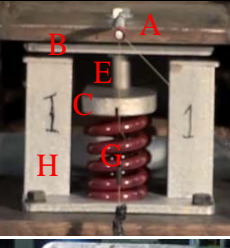
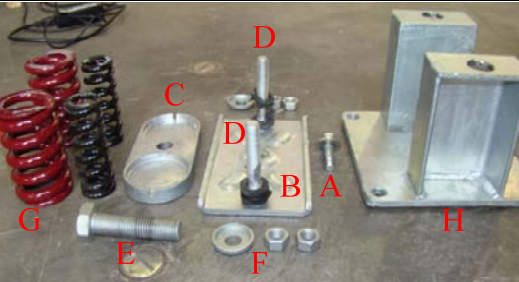
In order to investigate the seismic performance and proper seismic restraint strategy of a spring isolated generator, cyclic loading tests and shaking table tests were carried out for the generator with spring isolated system (I/ system) and Isolation/Restraint system (I/R system).

3.1. Test Specimen

As shown in Table 3.1, a 600kW diesel generator was used as the test specimen. The generator was installed on a base frame to support the integrity of mechanical components and associated links. I/ system and I/R system were designed according to the operating frequency and weight of the generator by some Taiwanese manufacturer. I/ system was composed of four spring isolators, and the I/R system was composed of I/ system and additional four snubbers. As shown in Table 1, the spring isolator can be separated into eight parts. Component A and B are used to connect equipment to the isolated system. Component C and E are used to transfer vertical loading to the springs. Component D, F and H are designed to prevent extremely large vertical vibration whenever the engine of isolated equipment was started. Due to the lack of lateral resistance mechanism, lateral gaps exist among various components. One is a 6mm gap filled with an unfixed thin rubber pad between the vertical restraint rod and restraint base. The other is a 2mm gap between the top hex-head bolt and top plate. These two components are connected with a washer to resist the shear force by friction.

Corresponding to the installation in practice, I/ and I/R system were arranged outside the base frame to lower the center of mass of generator. As shown in Fig. 3.1, spring isolators and snubbers were anchored through stiffened plates and connection plates, which were welded to the base frame. In cyclic loading tests, the actuator was also connected to the base frame.

Table 3.1. Test specimen and components of the associated I/R system.

Diesel generator	Spring Isolator Components	
 <p data-bbox="252 510 539 539">5.5ton/3.8m*1.55m*2.2m</p>		
<p data-bbox="347 555 443 584">Snubber</p>		<p data-bbox="842 562 1297 591">Loading/static deflection: 2400kgf /2.5cm</p> <p data-bbox="842 591 1281 620">A and B: top hex-head bolt and top plate</p> <p data-bbox="842 620 1273 649">D and F: vertical restraint rods and nuts</p> <p data-bbox="842 649 1201 678">C and E: load plate and load bolt</p> <p data-bbox="842 678 962 707">G: springs</p> <p data-bbox="842 707 1026 736">H: restraint base</p>

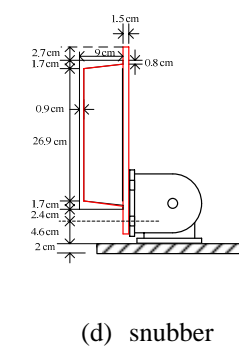
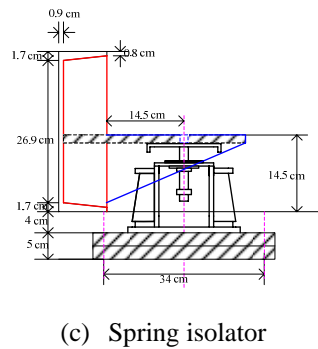
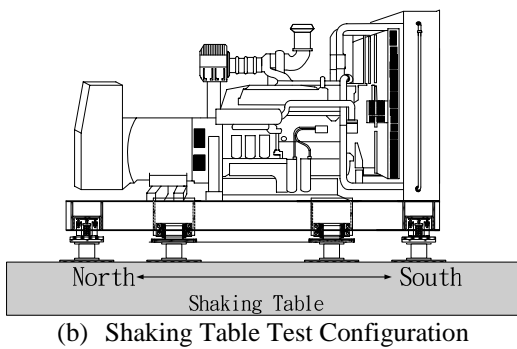
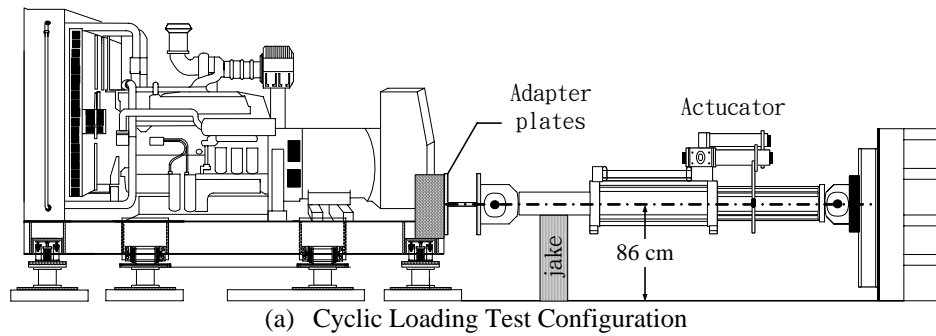
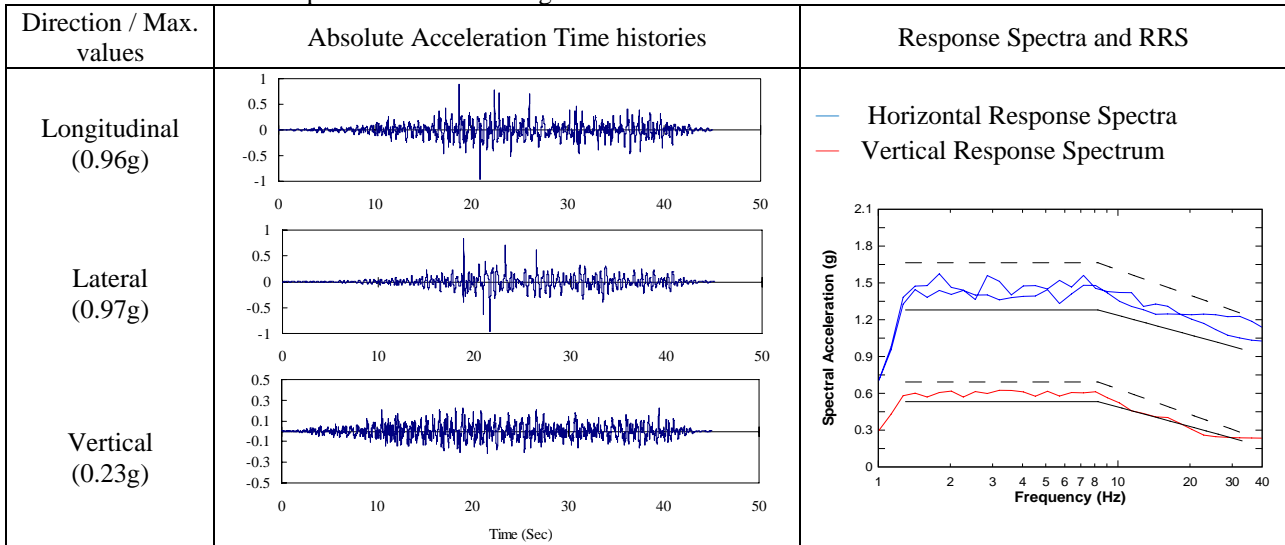


Figure 3.1. Test arrangement and connection details

3.2. Test Procedure

In cyclic loading tests, input motions were displacement controlled and divided into two parts to avoid unpredictable damage happened to the base frame. Considering the gap between restraint rods and restraint bases of spring isolators, a triangular displacement wave form with a increment of 0.5mm after every 2 cycles are used during the “unrestrained stage”. Then, the displacement increment of 2.5mm was imposed in every 2 cycles after the restraint rods touched to restraint bases. The Cyclic load tests were executed at a speed of 0.5 mm/sec until spring isolators were damaged. On the other hand, tri-axial artificial input motions of shaking table tests were generated by keeping the same phase spectra of CHY009 stations recorded during the 1999 Chi-Chi Taiwan earthquake, and compatible with associated design horizontal and vertical spectra. Table 3.2 depicts maximum values, response spectra and RRS of the tri-axial artificial input motions at roof level.

Table 3.2. Artificial input motions of shaking table tests.



4. TEST RESULTS

4.1. Damage States

From the test results, spring isolators were damaged due to the failure of the connections between vertical restraint rods and top plates. As shown in Table 3.1 and Table 4.1, vertical restraint rods and top plates were shallowly thread connected. In the cyclic loading test for the generator with I/ system, the connections were loosened under small a horizontal displacement. The threads of connections were completely worn out at the end of the test and caused the restrained rods separated from the top plates. The test was stopped until restrained rods of three spring isolators were damaged. The same damage mechanism of spring isolators was also observed in the shaking table test under 100% of the tri-axial artificial motion at roof level. For the cyclic loading test for the generator with I/R system, spring isolators remained in the elastic stage, and the vertical restraint rods were still in place.

Table 4.1. Observed damage states from test results.

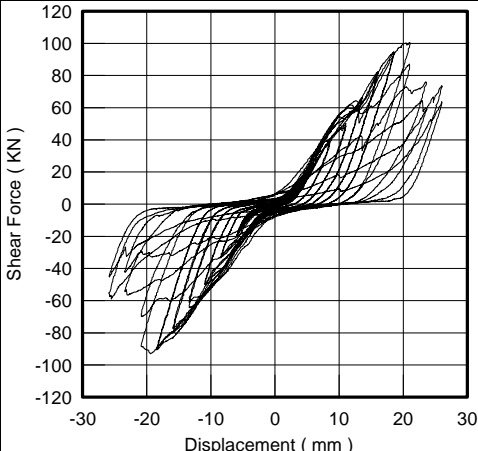
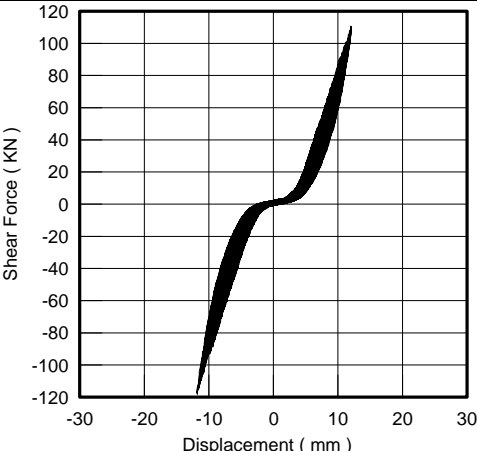
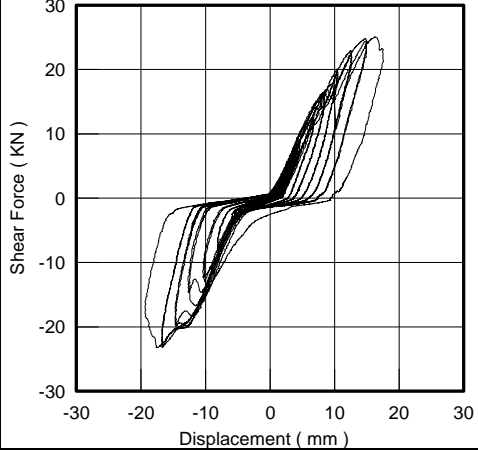
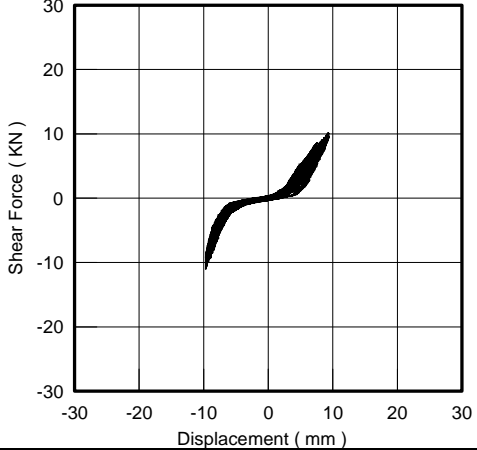
Cyclic loading test results: generator with I/ system	
<p>● Damage ● Loose</p>	
Shaking table test results: generator with I/ system 100% tri-axial artificial motion (at roof level)	
<p>● Damage ● Loose ○ Fixed</p>	

4.2. Cyclic Loading Tests

Table 4.2 depicts the horizontal input motions of the actuator and responses of I/ and I/R systems during cyclic loading tests. The maximum lateral displacement of the generator with I/ system was about 21.0 mm when the isolation system achieved the maximum shear forces during the cyclic loading tests. To avoid unpredictable damage to the base frame, the test for I/R system was only executed up to the force (118.1kN) slightly larger than the force applied to the test of I/ system (100.6kN). The generator with I/R system remained in the elastic range, and the corresponding displacement of about 11.8 mm due to constraint by the snubbers.

To obtain detailed seismic behavior of spring isolators, the force-displacement curves of the spring isolators when they achieved the maximum shear force were further discussed. Figure 4.1 compares the force-displacement curves of spring isolators at the southeast corner in I/ and I/R systems. Plot (a) depicts the inelastic behavior of I/ system resisting the maximum shear force while I/R system remains mainly in the elastic range under the same maximum force as shown in plot (b). The elastic behavior of the spring isolator can be separated into two parts. In the first part (i.e. H-A-B and F-E-D lines in plot (b)), the lateral stiffness is mainly supplied by springs. In the second part (i.e. B-C-D and H-G-F lines in plot (b)), the gaps between vertical restraint rods and restraint base of the spring isolator are closed. The lateral stiffness becomes larger due to the engagement of the vertical restraint rods. As mentioned above, the inelastic response of spring isolator was mainly caused by the damage of connections between restrained rods and its top plate. It is noted that negative stiffness behavior occurs (i.e. C-D and H-I lines in plot (a)) while shear force exceeds the friction force between the top hex-head bolt and the top plate, and sliding occurs between the two components.

Table 4.2. Input motion and responses in cyclic loading tests.

		Test 1 (I/ system)		Test 2 (I/R system)	
Actuator					
Test 1	Test 2				
Maximum Shear Force (kN)					
100.6	118.1				
Corresponding Displacement (mm)					
21.0	11.8				
One Spring Isolator (SE)					
Test 1	Test 2				
Maximum Shear Force (kN)					
50.1	22.1				
Corresponding Displacement (mm)					
16.4	9.8				

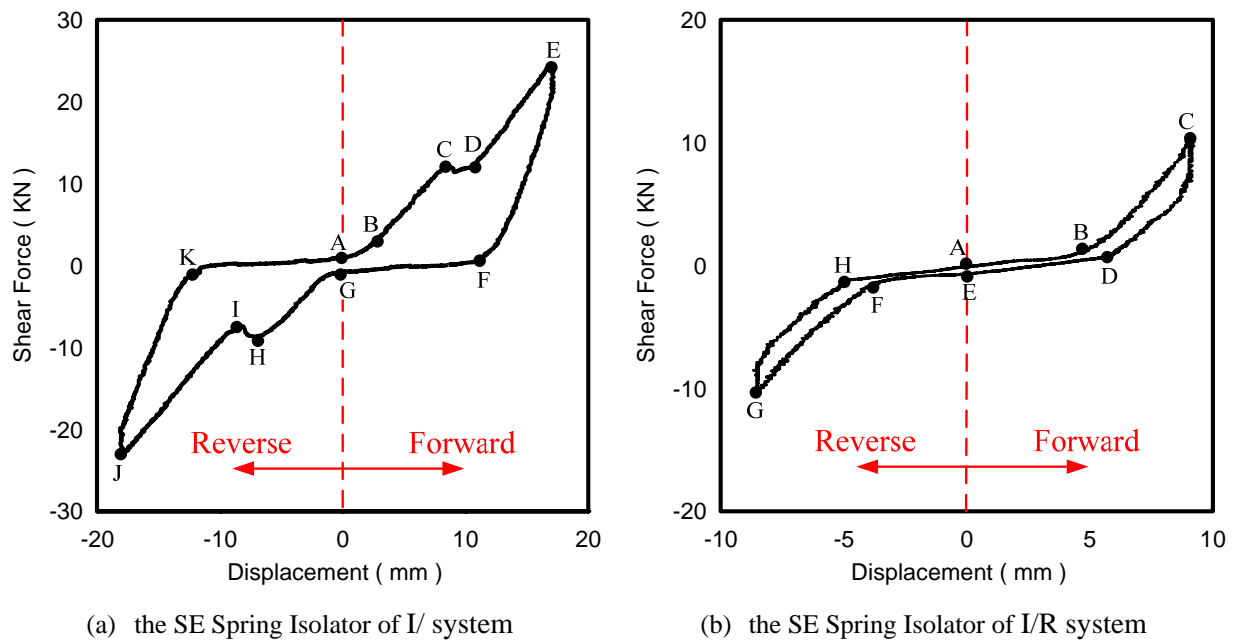


Figure 4.1. Force-displacement curves of spring isolators of I/ or I/R systems

4.3. Shaking Table Tests

4.3.1. Dynamic characteristics of isolated equipment

In shaking table tests, system identification was executed by both impulse tests and sine sweep tests. Table 4.3 illustrates the results of system identification tests for I/ and I/R systems. Since the snubbers were provided as the horizontal restraint components for I/R system, the fundamental frequencies in horizontal directions of I/R system are larger than those of I/ system. The snubbers in I/R system were designed to accommodate the vertical movement by a hinge mechanism. Therefore, under small excitation in the system identification tests, the fundamental frequency in the vertical direction of I/R system is just slightly larger than those of I/ system.

Equivalent viscous damping ratio of both I/ and I/R system were obtained by recording the decaying rate of free vibration. As shown in Table 4.3, the free vibration of I/R system has a faster decaying rate than that of I/ system due to the restraint rubber pads of snubbers. The equivalent damping ratio in each direction of I/R system was larger than that of I/ system.

4.3.2. Acceleration and Rocking Response

In the artificial motion tests, the generator with I/ system were damaged under a 100% tri-axial artificial motion at roof level. Table 4.4 depicts the force-displacement curves of spring isolators at the southwest corner of I/ and I/R system under tri-axial artificial motion tests. The spring isolator of I/ system shown in Table 4.4 is slightly damaged with loosened vertical restraint rods. The shear force-displacement curves of the spring isolator of I/ system shows similar inelastic behavior to cyclic loading test results. The vertical force-displacement curve of the spring isolator showed that the damage of the connection between the vertical restraint rods and the top plate also slightly affected its vertical response.

Compared with I/ system, the dynamic responses of the spring isolator of I/R system remained essentially in elastic stage in the tri-axial artificial motion test. Its lateral force-displacement curves showed that horizontal responses were mostly in the first part of the elastic stage due to the constrained lateral displacements by snubbers.

Table 4.3. System Identification results of I/ and I/R systems

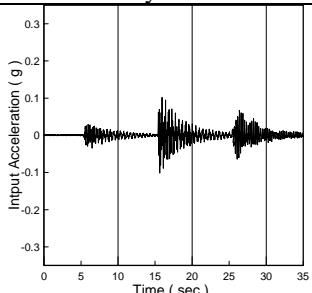
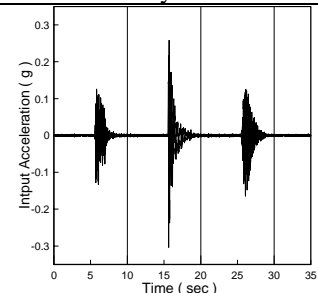
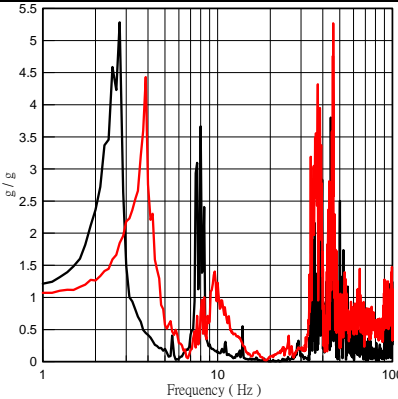
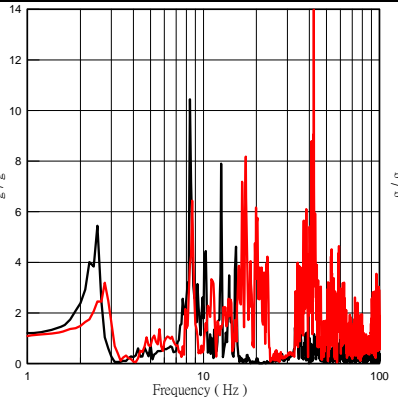
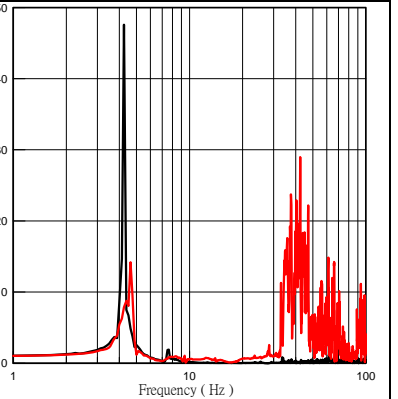
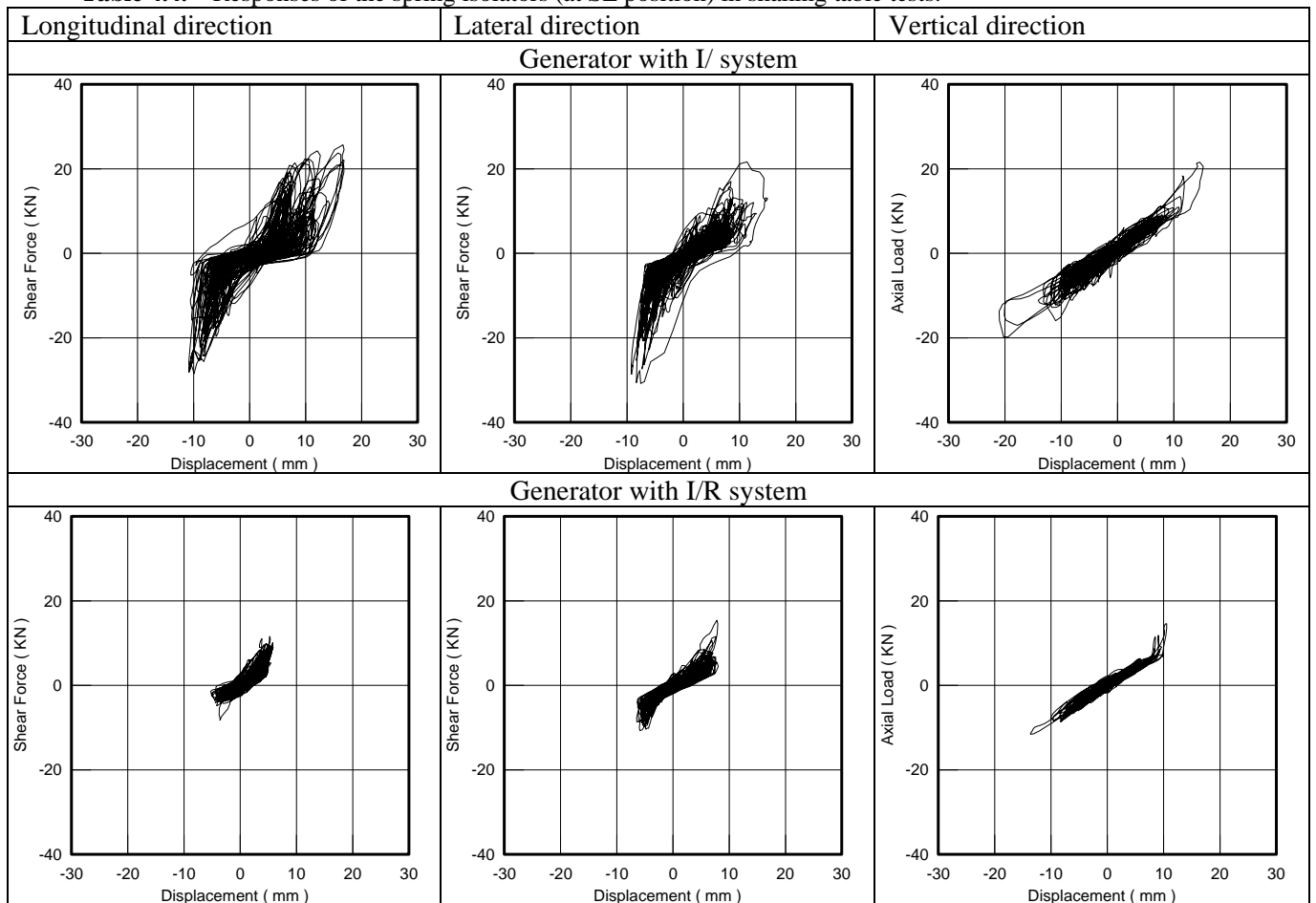
	I/ System			I/R system			Lateral response in impulse tests		
	Long.	Lat.	Vert.	Long.	Lat.	Vert.	I/ System	I/R system	
Fundamental frequency (Hz)	2.75	2.5	4.38	3.88	2.75	4.63			
Equivalent damping ratio (%)	2.76	2.72	1.04	6.85	6.15	3.28			
Transfer Function I/ — I/R —									
	Longitudinal Direction			Lateral Direction			Vertical Direction		

Table 4.4. Responses of the spring isolators (at SE position) in shaking table tests.

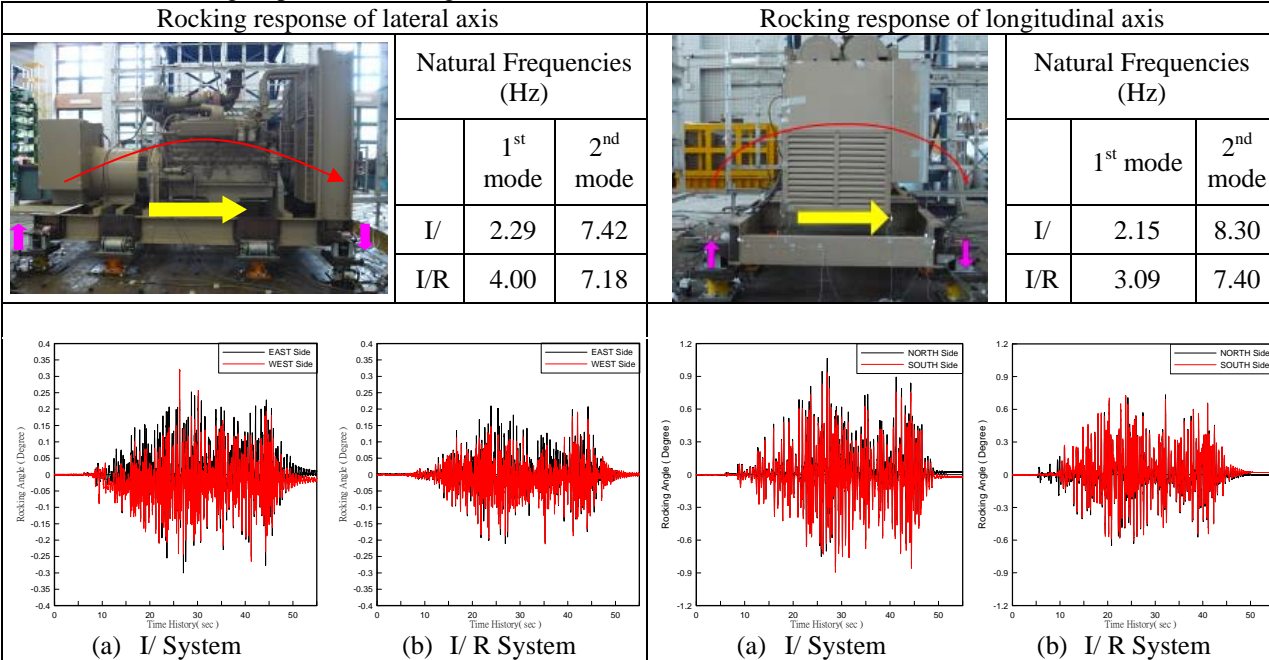


Shown in Table 4.5, transmissibility factor which is defined as the ratio of the peak value of acceleration response to the peak value of input motion was used as an index to compare the acceleration response of I/ and I/R systems in the artificial input motion tests. In the artificial motion tests, due to restraint rubber pads of snubbers, transmissibility of I/R system were much higher than that of I/ system except for the longitudinal uni-axial tests. In addition, the extremely high magnification values were observed in the vertical direction for both systems. This is caused by the impact between the restraint nut and restraint base of spring isolators of I/ system, and the partial constraint of vertical movement by the snubbers of I/R system. Beside the translational movements, rotational responses were also observed in the shaking table tests. Table 4.6 illustrates the natural frequencies of rocking motion from the system identification tests and rotation angle response under the 100% tri-axial artificial motion at roof level. Similar to the translational responses, the fundamental frequencies of rocking modes of I/R system were larger than I/ system. However, the rotation angle response, which is defined as the relative vertical displacement of two isolators divided by the distance of the two spring isolators, was limited by I/R system.

Table 4.5. Transmissibility values in shaking table tests

		Generator with I/ system				Generator with I/R system			
Measuring Direction	Isolator Position	Uni-axial test			Tri-axial test	Uni-axial test			Tri-axial test
		Long.	Lat.	Vert.		Long.	Lat.	Vert.	
Long.	SE	2.294	0.921	2.303	1.595	1.705	2.012	5.342	3.089
	NW	2.006	0.832	1.908	2.265	2.636	1.678	7.837	2.899
Lat.	SE	0.999	2.041	2.739	3.291	0.630	3.692	6.128	2.606
	NW	0.858	3.000	2.994	3.342	0.616	4.044	6.917	3.354
Vert.	SE	1.979	2.602	8.951	16.676	1.587	3.945	13.161	15.533
	NW	2.385	2.046	8.308	10.476	2.010	3.594	9.163	14.700

Table 4.6. Rocking response in shaking table tests



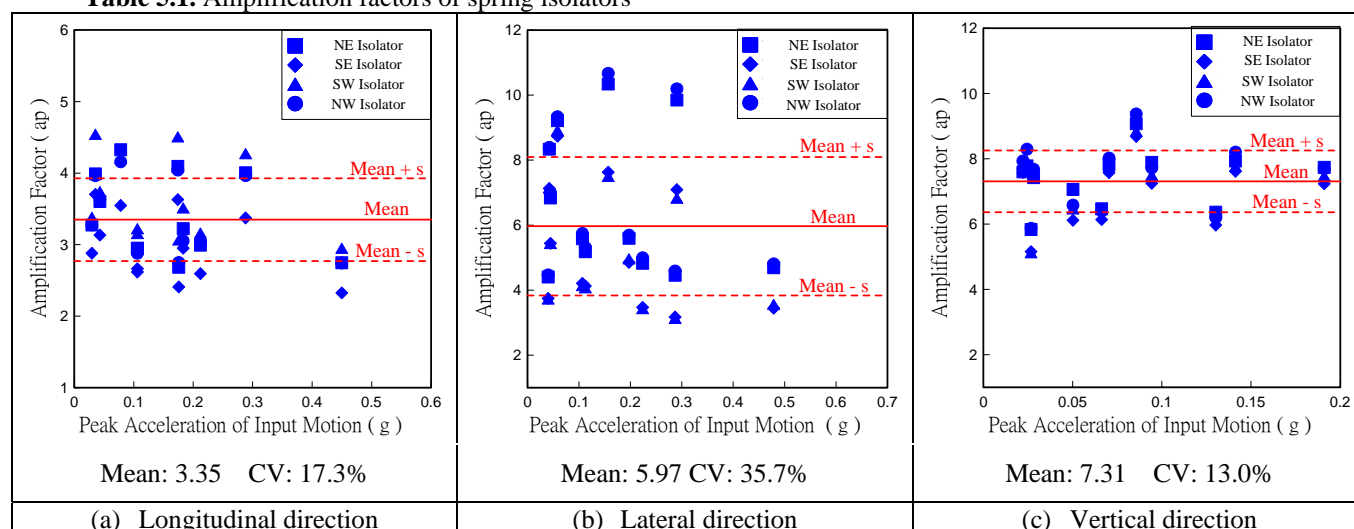
5. COMPARISON WITH DESIGN CODES

In this paper, the amplification factor of the seismic design force of spring isolated equipment is defined as the ratio of the root mean square (RMS) of acceleration response history to the RMS of the input acceleration history. The amplification factors are calculated from the small to middle intensity shaking table tests, in order to ensure I/ and I/R systems remain in the elastic range.

In ASCE 7-10, the component amplification factor, a_p , can be determined by the flexibility of the

component and attachments. According to the system identification test results, spring isolated generator should be considered as a flexible component since fundamental frequencies in three directions were all smaller than 16.6Hz. As mentioned above, the component amplification factor a_p for spring isolated components is 2.5 in both TBC and ASCE 7-10. However, according to shaking table test results, most a_p values of I/ system exceed 2.5. As shown in Figure 4, due to nonlinear behavior in the dynamic response, such as lateral gaps among isolator components, sliding response of spring, and impact response due to bumps between restraint nuts and restraint base of spring isolators, coefficient of variation were quite large in the three directions.

Table 5.1. Amplification factors of spring isolators



6. CONCLUSIONS

In this paper, cyclic loading tests and shaking table tests for the spring isolated generator were summarized. From test results, the major failure mode of spring isolators was due to the damage of connections between vertical restraint rods and top plates. The hysteretic responses of spring isolators were characterized from cyclic loading tests. In shaking table tests, extremely high vertical acceleration responses occurred in both I/ and I/R systems, which were induced by the impact response among the components of spring isolators in I/ system and by the partial constraint from the vertical movement of snubbers in I/R system. Most amplification factors obtained from shaking table tests were much larger than those specified in design codes. Overall, this study points out the needs for improving the earthquake resistant mechanism of spring-isolated components.

ACKNOWLEDGEMENT

This support of the National Science Council (NSC) under the Grants NSC99-2625-M011-002 is gratefully acknowledged

REFERENCES

- J.S. Hwang and I Chen. (2009). Experimental study on seismic behavior of vibration isolation bearings of electrical and mechanical systems of hospitals, Master Thesis, National Taiwan University of Science and Technology. (in Chinese)
- Ministry of the Interior. (2011). Taiwan Building Code: Seismic Design Specifications and Commentary of Buildings, Ministry of the Interior, Taiwan. (in Chinese)
- American Society of Civil Engineers. (2010). Minimum Design Loads for Buildings and Other Structures, ASCE/SEI 7-10, ASCE, Virginia, U.S.
- ICC Evaluation Service inc. (2007). AC156: Acceptance Criteria for Seismic Qualification by Shake-table Testing of Nonstructural Components and Systems, ICC Evaluation Service inc., U.S.